"Surface Dislocation" Process for Surface Reconstruction and Its Application to the Silicon (111) 7×7 Reconstruction

P. M. Petroff and R. J. Wilson[a]
Bell Laboratories, Murray Hill, New Jersey 07974

(Received 25 March 1983)

The silicon (111) 7×7 surface reconstruction has been observed by surface-sensitive transmission-electron microscopy. The topography of the reconstructed surface is accounted for by the cooperative motion of surface atoms over large areas via a new process involving the generation of "surface dislocations" to relieve the backbond-induced surface stresses.

PACS numbers: 68.20.+t, 61.16.Di

In recent years a large number of experimental results on the Si (111) 7×7 reconstructed surface have suggested or demonstrated the existence of triangular structural features for the unit cell of the reconstructed surface.[1-3] Theoretical models have attempted to incorporate these results by considering the variation of surface energy with changes in atomic bonding which accompany the 7×7 reconstruction.[4-6] No model has, to our knowledge, attempted to account for the role of surface steps in the nucleation kinetics of the 7×7 structure from the 1×1 Si (111) phase. Perhaps the most important experimental results on this subject are those of Osakabe, Yagi, and Honjo[7] and Yagi, Takayanagi, and Honjo[8] who directly observed by reflection-electron microscopy the nucleation of the 7×7 phase at step edges and its growth towards the step risers. These important results bear heavily on the mechanism of the reconstruction and should be considered in any structural model of large superlattice cells.

In this Letter, we propose a new surface-reconstruction process which accounts for the cooperative motion of surface atoms over large areas and explains the observed results on the nucleation kinetics.[7,8] The two guiding ideas behind the proposed mechanism are the following: (1) The surface is a highly anisotropic medium which, by analogy to crystalline solids with the largest elastic anisotropy constant (e.g., lithium, β brass), will tend to exhibit crystallographic phase transformations to achieve a lower-energy state. (2) The phase transformation we invoke for the surface reconstruction takes place via the generation of surface defects to lower the surface misfit strain energy. As pointed out by Phillips,[4] this misfit strain energy may play an important role on the energetics of the surface reconstruction. The model developed in this Letter is supported by new experimental data which we have obtained using a surface-sensitive transmission-electron-microscopy (SSTEM) technique to analyze the Si (111) 7×7 reconstruction.

The recently developed SSTEM technique[8,9] is used in this investigation. Briefly, the SSTEM is carried out with use of a conventional transmission-electron microscope which has been converted to operate with a UHV environment around the sample. The sample is cleaved from a Syton-polished Si (111) As-doped (0.001-Ω-cm) wafer to produce a bar with dimensions $5\times3\times0.5$ mm^3. A small hole (diameter $\cong 1$ mm) is then etched chemically with a mixture of HF, HNO_3, and H_3PO_4 from one of the surfaces. The sample is precleaned by use of a previously developed procedure.[10] After insertion in the transmission-electron microscope (TEM), the surface preparation and sample thinning are carried out by dc resistive heating under UHV conditions in a specially built sample holder.[9] We find in general that heating of the sample to the point where the thinnest part of the sample melts is needed to produce a Si surface free of silicon carbides (as detected by imaging and diffraction in TEM). To minimize inelastic scattering, absorption, and dynamical diffraction effects from the bulk of the thin film, the sample is thinned to $\cong$ 100–200 Å by controlled evaporation during imaging in the transmission mode with an electron beam of 200 keV energy. The 7×7 reconstruction is obtained after cleaning the sample and lowering the sample temperature to $T \lesssim 750$ °C. Figure 1(a) gives the essential features of the Si 7×7 transmission-electron diffraction pattern (TED) for a sample oriented such that the e beam is approximately normal to the surface. Figure 1(b) shows the diffracted intensities as measured with a spot densitometer. The TED pattern indexing in Figs. 1(a) and 1(b) are based on a cubic-axis primitive cell and hexagonal-axis primitive cell (surface notation), respectively. The symmetry of the

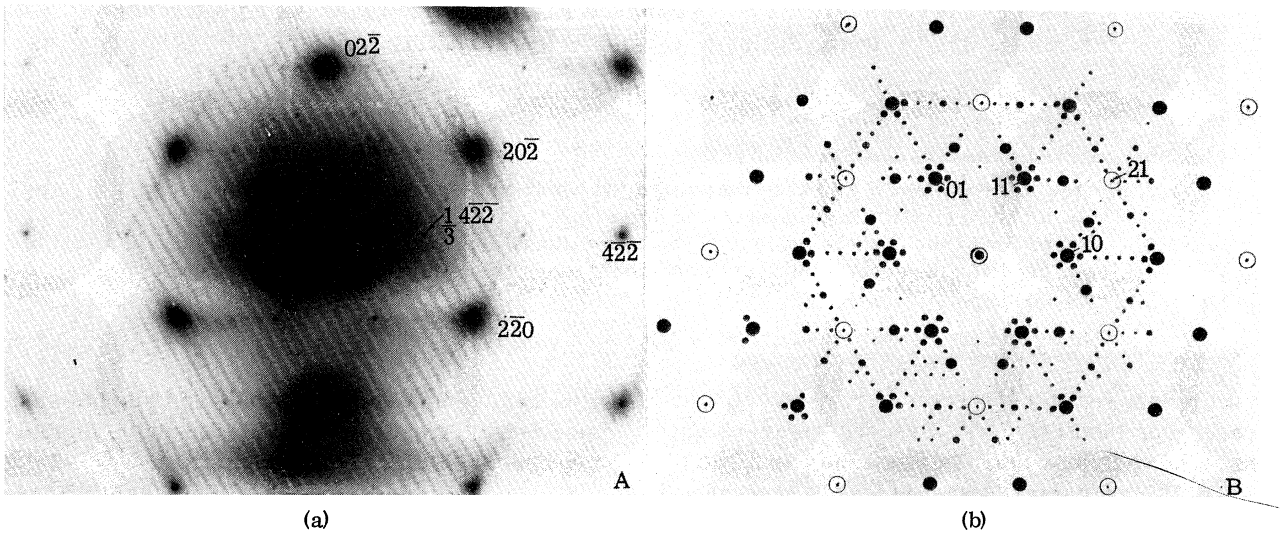

(a) (b)

FIG. 1. (a) TED pattern of the Si (111) 7×7 reconstructed surface ($T=350\,^{\circ}\mathrm{C}$). Silicon surface and bulk spots are indexed in the cubic-axis notation. (b) Schematic rendering of the intensity distribution on the TED pattern in (a). As indicated by the size of the spots, five levels of intensities have been measured. Surface spots are indexed in the hexagonal surface notation. Open circles indicate bulk diffraction spots.

pattern is threefold with additional reflection around the $\langle 21\rangle$ directions. This results in a sixfold symmetry of the TED pattern. The surface-spot periodicity along the $\langle 11\rangle$ and $\langle 10\rangle$ directions corresponds to a real-space period of $7d_{(110)}$.

The changes in surface topography during the reconstruction are shown in the dark-field electron micrographs taken with a $\langle 220\rangle$-diffracted beam along with the six neighboring surface-diffracted beams. The characteristic feature which is observed consists of triangular domains with sides parallel to $\langle 110\rangle$ and sizes in the range $\cong 75$ to 1500 Å. The imaging spatial resolution was limited by instrumental problems to $\cong 50$ Å in these experiments. Contrast experiments indicate that the side of the triangle parallel to the operating $\langle 220\rangle$ Bragg reflection is invisible while the two other sides have opposite contrast (Fig. 2). This contrast is consistent with a defect-induced strain field oriented along $\langle 111\rangle$ directions inclined at 70.53° to the (111) surface at the edges of the triangular domains. The defects most likely to produce this type of contrast are stacking faults or antiphase boundaries or boundaries between reconstructed and unreconstructed parts of the surface. These defects constitute the first evidence that stacking-fault–type defects and thus dislocations are generated during the reconstruction. Although the relationship between the 7×7 reconstruction is not directly observable in Fig. 2, we note that these triangular features and the reconstructed surface-diffraction spots in the TED disappear when the surface becomes contaminated (through loss of UHV environment) or is heated through the 7×7 to 1×1 phase transition.

The $\langle 10\rangle$ and $\langle 01\rangle$ diffraction spots in Fig. 1(b) are normally forbidden for kinematic diffraction conditions because of the cancellation of the diffracted wave amplitudes for three successive double (111) layers in the unit cell.[11] They may, however, appear in the following cases: (a) for smooth surfaces spaced by a number of double

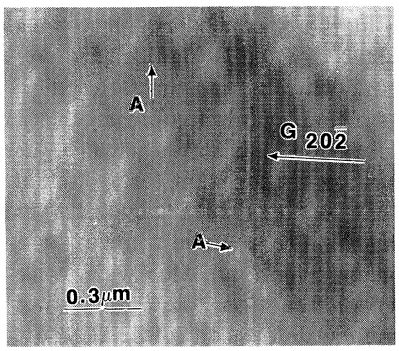

FIG. 2. Dark-field TEM micrograph of the reconstructed surface at $T=350\,^{\circ}\mathrm{C}$. The operating Bragg reflection includes the $(20\bar{2})$ beam and six adjacent surface beams. Triangular domains (A) are characteristic of the 7×7 reconstructed surface.

layers not equal to a multiple of three; (b) for rough surfaces with surface steps[12]; or (c) for stacking faults parallel to the surface. Finally, we also remark that a surface step with height $d_{(111)} = 3.14$ Å is produced by the glide of a dislocation with Burgers vector $\vec{b} = \frac{1}{2}a\langle 110\rangle$ on a $\{111\}$ plane inclined to the surface. Thus, the most intense surface reflections, i.e., (10), (11), and (01) spots in the TED pattern in Fig. 1 may be accounted for by three different lattice transformations.

For the purpose of explaining the surface reconstruction we choose the crystallographic transformation which will remove the maximum stress between the surface layer and the underlying substrate. By analogy with the case of strained interfaces where the misfit strain is accommodated by misfit dislocations originating from the surface, we propose that the formation of the 7×7 reconstructed surface proceeds by the generation of "surface dislocations."[13] For this reconstruction we require three sets of surface dislocations with Burgers vectors $\vec{b} = \frac{1}{2}a \times \langle 110\rangle$ originating from the step edges at the surface and moving towards the step risers by glide along $\langle 110\rangle$ directions on the (111) planes inclined to the surface (Fig. 3). Since we require these dislocations to be parallel to the surface and to accommodate the maximum misfit strain, their Burgers vector makes an angle of 60° with the dislocation line. To produce the desired periodicity in the pattern and follow the energy minimization scheme proposed by Pandey,[5] the surface dislocations are generated every eighth $\{111\}$ plane [Fig. 3(b)]. The three sets of shear operations are generated by use of the following rules. First, adjacent pairs of 60° surface dislocations with Burgers vectors $\vec{b}_1$ and $\vec{b}_2$ producing two adjacent surface steps of heights $d_{(111)} = 3.14$ Å are introduced. A second and third set of 60° dislocations with Burgers vectors $\vec{b}_3, \vec{b}_4$, and $\vec{b}_5, \vec{b}_6$, respectively, are generated. These sets of dislocations have Burgers vectors producing surface steps of height $-d_{(111)}$. The crossing of two surface steps with opposite height, $\pm d_{(111)}$, yields a feature with height equal to that of the original surface step [Fig. 3(b)]. As seen in Fig. 3(b), the reconstructed surface consists of equilateral triangular islands and equiside parallelograms along the three $\langle 110\rangle$ directions in the (111) plane. The sides of these islands have length equal to $7d_{(110)} = 26.8$ Å and their height is $\pm nd_{(111)}$, with $0 \lesssim n \lesssim 2$, with respect to the original surface. The apex of each island coincides with the intersection of two or three dislocation cores and thus it is expected that a deep hole in the surface will be present at these points. If we assume that the dislocation cores are reconstructed[14] by forming five-, six-, and seven-membered rings, the surface dislocations will not introduce a large additional number of dangling bonds except perhaps at the apex of the surface islands. The calculated TED pattern based on this unit cell and with use of the kinematical diffraction approximation exhibits seventh-order diffraction spots.[15] A detailed computed TED pattern taking into account possible dimerization effects[2] will be published later.

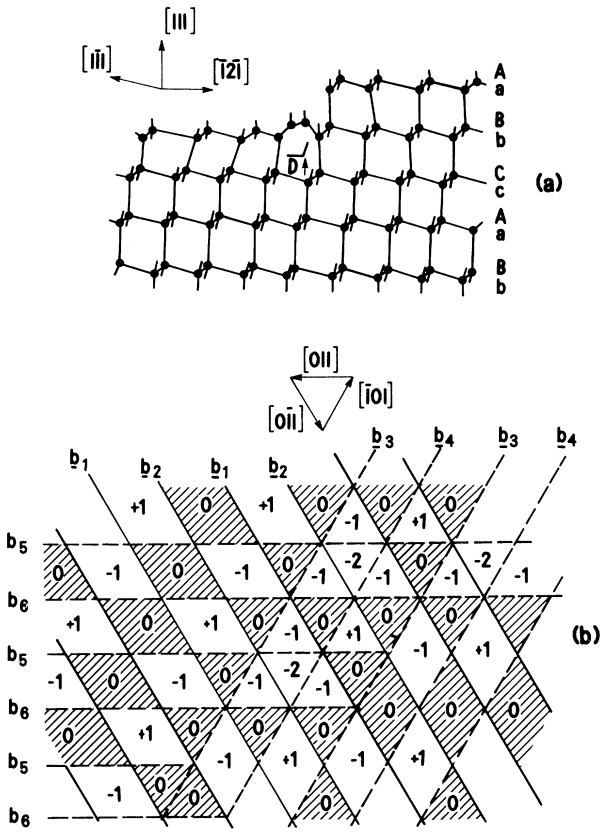

FIG. 3. (a) Schematic projection on a $(10\bar{1})$ plane of the surface step created by the introduction of a 60° "surface dislocation" on a $(1\bar{1}1)$ plane intersecting the (111) surface. The dislocation core is shown reconstructed in *D*. (b) Schematic projection on the (111) plane of the surface topography produced by three sets of $\langle 110\rangle$ dislocations. The various levels of the surface for each island have been indicated by numbers corresponding to a multiple of 3.14-Å (see text) displacement along the (111) normal. The Burgers vectors are $\vec{b}_1 = \frac{1}{2}a[101]$, $\vec{b}_2 = \frac{1}{2}a[\bar{1}\bar{1}0]$, $\vec{b}_3 = \frac{1}{2}a[0\bar{1}1]$, $\vec{b}_4 = \frac{1}{2}a[110]$, $\vec{b}_5 = \frac{1}{2}a[011]$, and $\vec{b}_6 = \frac{1}{2}a[\bar{1}01]$.

The surface-dislocation model requires a nucleation of the 7×7 phase at step edges and produces a roughening of the step edge due to the mixed character of the dislocation. Both features are consistent with the reflection-electron-microscopy results.[7,8] The transformation from the 7×7 into the 1×1 phase at higher temperature ($T_c \gtrsim 800\,^{\circ}\mathrm{C}$) would take place by a reverse motion of surface dislocations and/or annihilation at the surface. The dependence of the dislocation core energy on impurities[16] is expected to influence the dislocation mobility and thus the surface-dislocation model could account for the reported impurity dependence[17,18] of the Si (111) 5×5 surface reconstruction below 600 °C.

In conclusion, the concept of surface dislocations, which has been introduced to account for the cooperative motion of surface atoms over large areas during the Si (111) 7×7 reconstruction, may indeed be useful for other surfaces which reconstruct with large unit cells and for materials with large backbond stresses.

We wish to acknowledge helpful discussions with J. C. Phillips and E. G. McRae.

---

[a]Present address: IBM Research Laboratory, 5600 Cottle Road, San Jose, Cal. 95193.

[1]M. J. Cardillo, Phys. Rev. B 23, 4279 (1981).

[2]E. G. McRae and C. W. Caldwell, Phys. Rev. Lett. 46, 1632 (1981); E. G. McRae, to be published.

[3]G. Binnig, H. Rohrer, Ch. Gerber, and E. Weibel, Phys. Rev. Lett. 50, 2, 120 (1983).

[4]J. C. Phillips, Phys. Rev. Lett. 45, 11, 905 (1980).

[5]K. C. Pandey, to be published.

[6]L. C. Snyder, Z. Wasserman, and J. M. Moskowitz, J. Vac. Sci. Technol. 16, 1266 (1979).

[7]N. Osakabe, K. Yagi, and G. Honjo, Jpn. J. Appl. Phys. 19, L309 (1980); N. Osakabe, Surf. Sci. 109, 353 (1981).

[8]K. Yagi, K. Takayanagi, and G. Honjo, *Crystal Growth, Properties and Applications* (Springer-Verlag, Berlin, 1982), p. 47.

[9]R. J. Wilson and P. M. Petroff, to be published.

[10]R. C. Henderson, J. Electrochem. Soc. 6, 772 (1972).

[11]D. Cherns, Philos. Mag. 30, 549 (1974).

[12]S. Iijima, Ultramicroscopy 6, 41 (1981).

[13]By analogy with the Volterra dislocation, the "surface dislocation" is defined by its direction and Burgers vector. As indicated by its name, it is located at the surface or within two atomic layers from the surface. Consequently, the core of the surface dislocation will reconstruct readily and its core energy should be smaller than that of the bulk dislocation.

[14]P. B. Hirsch, J. Phys. (Paris), Colloq. 40, C6-27 (1979).

[15]J. C. H. Spence and K. Takayanagi, to be published.

[16]H. Alexander, J. Phys. (Paris), Colloq. 40, C6-21 (1979).

[17]J. J. Lander, *Progress in Solid State Chemistry*, edited by H. Reiss (Pergamon, Oxford, 1965), Vol. 2, p. 26.

[18]E. Bauer, Vacuum 22, 539 (1972).

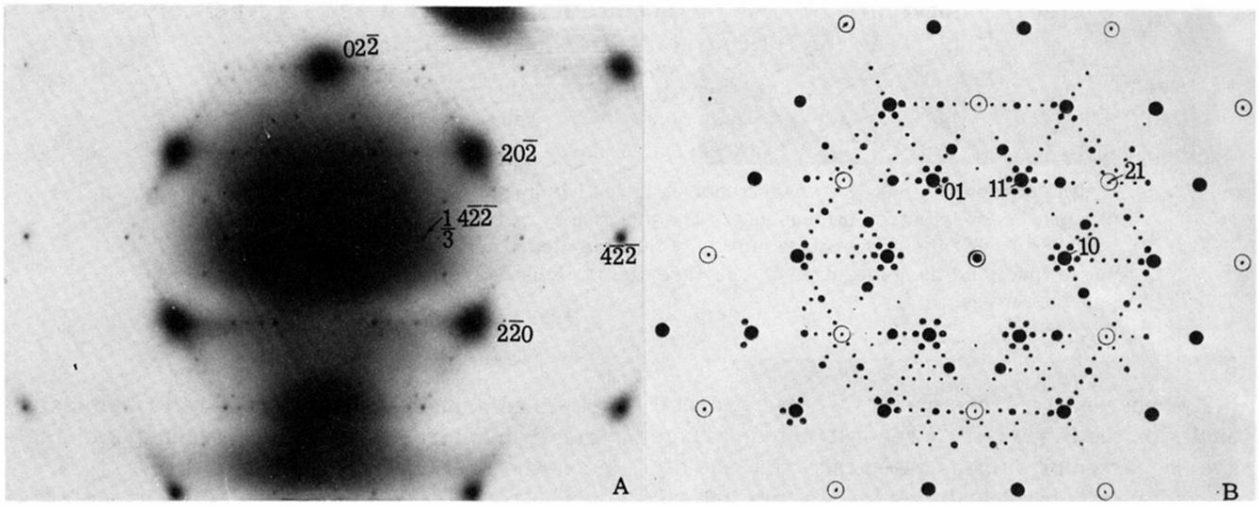

(a) (b)

FIG. 1. (a) TED pattern of the Si (111) 7×7 reconstructed surface ($T = 350\,^{\circ}\mathrm{C}$). Silicon surface and bulk spots are indexed in the cubic-axis notation. (b) Schematic rendering of the intensity distribution on the TED pattern in (a). As indicated by the size of the spots, five levels of intensities have been measured. Surface spots are indexed in the hexagonal surface notation. Open circles indicate bulk diffraction spots.

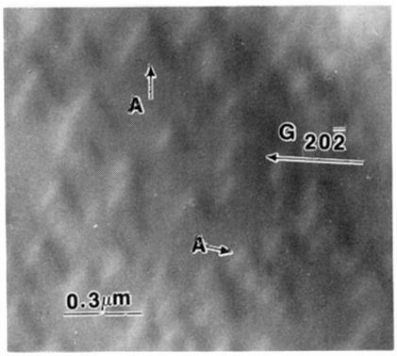

FIG. 2. Dark-field TEM micrograph of the reconstructed surface at $T = 350\,^{\circ}\mathrm{C}$. The operating Bragg reflection includes the $(20\bar{2})$ beam and six adjacent surface beams. Triangular domains (A) are characteristic of the 7×7 reconstructed surface.